Mario Bertero, Patrizia Boccacci, Gabriele Desiderà, Andrea La Camera, Marcel Carbillet, and Henri Lantéri

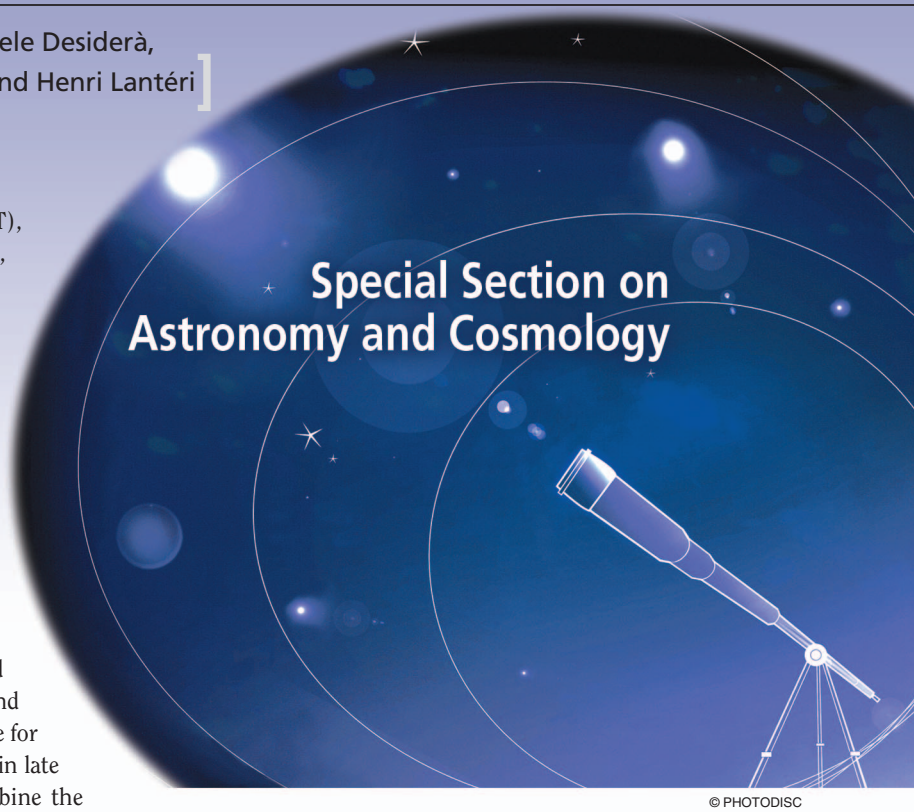

Imaging with LINC-NIRVANA

An introduction to deconvolution methods and their capability

The large binocular telescope (LBT), operating on the top of Mount Graham, Arizona, consists of two 8.4 m mirrors on the same mounting, with a distance of 14.4 m between their centers. First binocular light was achieved 6 March 2008 with the large binocular camera (LBC), consisting of two wide-field, high-throughput imaging cameras located at prime focus stations. Moreover, LBT will be equipped with a pair of 0.911 m adaptive secondary mirrors, each with 672 actuators.

One of the most innovative instruments of the LBT is the Fizeau interferometer, called LINC-NIRVANA (LN), which is in an advanced realization phase by a consortium of German and Italian institutions, led by the Max Planck Institute for Astronomy in Heidelberg. Installation is foreseen in late 2011. When operating, LN will coherently combine the beams coming from the two mirrors in a common focal plane (not in the pupil plane, as with essentially all existing interferometers), where interference then appears as spatial structure in the point-spread function (PSF) (for a discussion, see [1]). Direct imaging is provided in the wavelength range 1.0–2.4 μm (*J, H,* and *K* bands) on a wide field of view (FoV), thanks to its pyramid-based, layer-oriented multiconjugate adaptive optics (AO) system [2].

However, a single image of LN is characterized by an anisotropic resolution: the highest in the direction of the baseline joining the centers of the two mirrors, and the lowest in the orthogonal direction. This property implies the need of acquiring several images of the same target with different orientations of the baseline and to combine these images, by means of a suitable post-processing, to obtain a single image with improved resolution. Hence, LN will routinely require the use of image deconvolution methods. The purpose of this article is to provide a simple introduction to these methods and to illustrate their capability.

The PSF of the instrument will be the PSF of a single mirror modulated by the interference fringes, that are orthogonal to the direction of the baseline. Figure 1(a) shows the PSF in the ideal case, i.e., without optical and atmospheric aberrations; in Figure 1(b), we display the corresponding modular transfer function (MTF), showing the coverage of the u, v-plane provided by such a PSF. Therefore the band of the instrument, i.e., the domain in the u, v-plane where the MTF is not zero, consists

Digital Object Identifier 10.1109/MSP.2009.934714

1053-5888/10/$26.00©2010IEEE

essentially of three discs: the central one corresponds to the MTF of the 8.4 m mirror, while the side discs contain the additional information provided by the interferometer. This property implies that a single image of the interferometer is characterized by an anisotropic resolution: ideally, that of a 22.8 m mirror in the direction of the baseline (approximately 20 milliarcseconds (mas) in K-band) and that of a 8.4 m mirror (approximately 50 mas) in the orthogonal direction. However, thanks to Earth's rotation, it is possible to acquire images corresponding to different orientations of the same scientific object in the image plane. Since the instrument is not equipped with a large-angle derotation system, the fringes are always orthogonal to the baseline while the object is rotating in the FoV of the camera. This situation is illustrated in Figure 2. In Figure 2(a), we show the image of a binary in K-band, with magnitude $m = 20$, $\Delta m = 0$ and a separation of about 45 mas (hence resolved by a 22.8 m telescope), when its axis is parallel to the baseline; in Figure 2(b), we show the image of the same binary when its axis is orthogonal to the baseline. In such a case the resolution is that of a 8.4 m telescope and therefore the binary is not resolved.

As follows from the previous remarks, the basic problem of LN-imaging is to combine the different images for getting a single image, possibly with a resolution close to that of a 22.8 m mirror in all directions. This result can be hardly reached in practice because it depends on the level and uniformity of the AO correction and on the declination of the scientific target, controlling the orientations of the baseline that can be used during its observation (for a discussion, see [3]). In this article, we give a brief introduction to this problem. It can be solved by iterative methods related to the well-known Richardson-Lucy (RL) algorithm [4], [5]. Since RL is a particular case of the maximum likelihood method introduced by Shepp and Vardi [6] in emission tomography and denoted expectation maximization (EM), improvements of EM, proposed in the field of medical imaging can be applied to LN. For an introduction to methods of image reconstruction, see [7].

PREPROCESSING

The LN is equipped with a HAWAII-2 detector consisting of 2048×2048 pixels, thus producing, for each orientation of the baseline, a raw image of 4.2 megapixel. The pixel size is about 5 mas, so that the width of the corresponding FoV is about 10 arcsec. Since the diffraction limit of a 22.8 m telescope in K-band is 20 mas, this implies an oversampling by a factor 4 in this band.

A standard preprocessing of the raw images, consisting in correction for flat field, bad pixels, etc., must be performed. Moreover the background b, due to sky emission and dark current must be estimated but not subtracted; its value is one of the input parameters of the reconstruction algorithm.

The next step is the derotation of the images. This can be done in the physical space or in Fourier space [8]. After derotation the images are aligned, so that the object has exactly the same location in all the images. In Figure 3, we show the result of this preprocessing when applied to the images of Figure 2. We remark that, in the case of an arbitrary rotation angle, the rotated image is con-

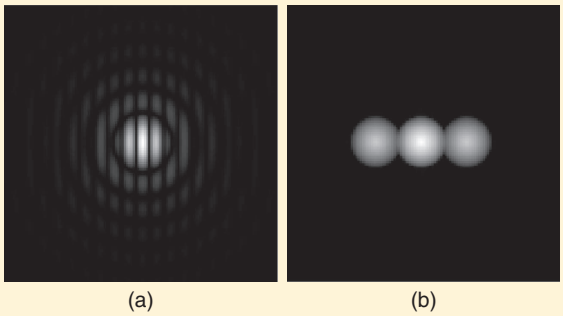

[FIG1] **(a) PSF and (b) MTF of LN.**

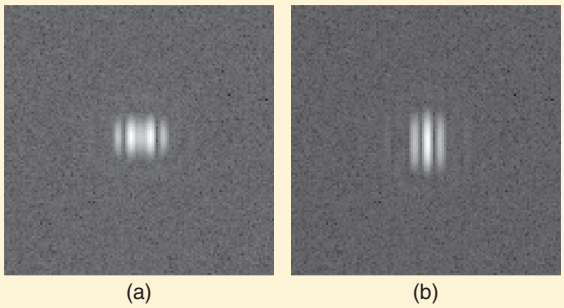

[FIG2] **Interferometric image of a binary star with the (a) axis parallel and (b) orthogonal to the baseline.**

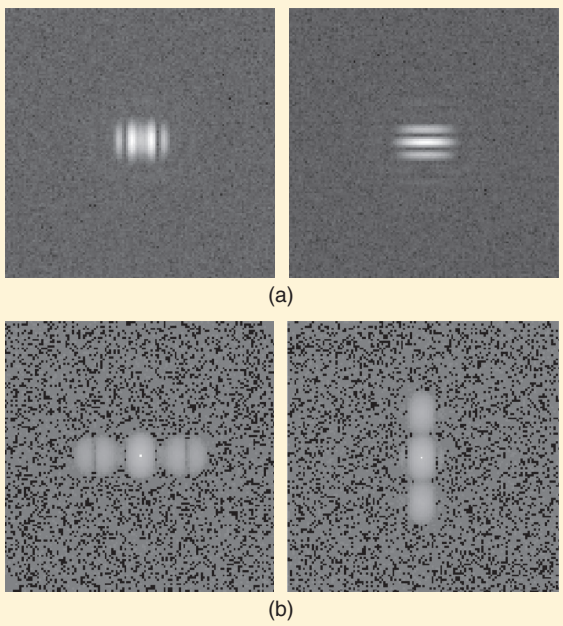

[FIG3] **(a) The same images of Figure 2 but with that to the right rotated by 90°, so that the binaries of the two images are aligned. (b) The modulus of the Fourier transforms of the images shown in (a). The additional information provided by the second image is evident, as well as the out-of-band noise due to the background.**

tained in a broader array; moreover different images can contain different parts of the same scientific object. This problem is also discussed in [8].

The last step is the estimation of the PSF. The AO system of LN will use natural stars as guide stars. If one or more stars are contained in the FoV, then the images of these stars can provide an estimate of the PSF. However, the extracted images may have a limited extent, because of surrounding objects, while the effect of the residual seeing, that is important in image deconvolution, may be significant on a broader region. For this reason, an extrapolation outside the extraction domain, based on a description of the seeing is also required. A procedure for extraction and extrapolation, based on a Lorentzian model, is described in [8]. In conclusion, at the end of the preprocessing step, for each image we have an estimate of the background and of the PSF. Moreover, the derotation ensures that the scientific object has exactly the same location in all images.

HOWEVER, THANKS TO EARTH'S ROTATION, IT IS POSSIBLE TO ACQUIRE IMAGES CORRESPONDING TO DIFFERENT ORIENTATIONS OF THE SAME SCIENTIFIC OBJECT IN THE IMAGE PLANE.

IMAGE RECONSTRUCTION

At the end of the preprocessing step, we have a set of p images, let us say $g_1, g_2, \ldots, g_p$, with the corresponding backgrounds $b_1, b_2, \ldots, b_p$ and PSFs $K_1, K_2, \ldots, K_p$. We assume that each PSF is normalized to unit sum of the pixel values. As one can easily understand by looking at Figure 3, with a relatively small number of images corresponding to equispaced angles between 0° and 180°, one can obtain a coverage of the Fourier plane corresponding essentially to that of a 22.8 m telescope. Unfortunately, such a situation can be hardly realized in practice.

THE BASIC ALGORITHMS

Even if we do not have a complete coverage of the u, v-plane, we can combine the p images to get a single restored image with a resolution that is uniform as far as possible. The first approach that comes to mind is to produce a single image g just by adding the p images and to reduce the problem to a single image deconvolution. If we take the arithmetic mean of the detected images, $g = (g_1 + \cdots + g_p)/p$, of the estimated backgrounds, $b = (b_1 + \cdots + b_p)/p$, and of the estimated PSFs, $K = (K_1 + \cdots + K_p)/p$, then we have the following model of image formation: $g = K * f + b$, where f is the unknown scientific target and the star denotes convolution. In this model, the flux of f coincides with the flux of $g - b$, thanks to the normalization of the PSFs. The deconvolution of the coadded image g is investigated in [9] and [10]. We can apply to this problem the modification of the RL-algorithm proposed in [11] for taking into account the background b; then the iteration is

$$f^{(k+1)} = f^{(k)} K^T * \frac{g}{K * f^{(k)} + b}, \tag{1}$$

where K^T denotes the "transposed" PSF, i.e., that obtained from K by reflection with respect to the central pixel. The quotient of images is intended pixel by pixel.

The iterations are, in general, initialized with a constant array, so that the result of the first iteration is basically a reblurring of the detected image. Moreover, as it is well known, early stopping of the iterations is required to avoid excessive noise propagation, at least in the case of extended scientific objects. It is also well known that, in the case $b = 0$, the flux of each iteration coincides with the flux of the coadded image g. If b is not zero, then numerical experience demonstrates that the flux of each iteration approximately coincides with the flux of $g - b$.

However, for faint objects, the result of the coadding in the u, v-plane is that the out-of-band noise of one image is added to the weak interferometric information contained in the side discs of another image, as one can easily understand by looking at the lower panels of Figure 3 and considering the addition of the two images in the u, v-plane. As a consequence the signal-to-noise (SNR) ratio is reduced in the side discs. Moreover, in the case of objects with a preferred direction, such as a binary, the flux in the coadded image has no directionality and is spread out over a broad region.

For these reasons, in [12], the case of multiple image deconvolution is considered and the modified version of the RL-algorithm for this problem is introduced. The iteration is now given by

$$f^{(k+1)} = \frac{1}{p} f^{(k)} \sum_{j=1}^{p} K_j^T * \frac{g_j}{K_j * f^{(k)} + b_j}. \tag{2}$$

We remark that, also in this case, when all the backgrounds are zero, the flux of each iteration coincides with the flux of the coadded image g, while approximately coincides with the flux of $g - b$ in the more general case.

ACCELERATION

The RL algorithm requires, in general, a large number of iterations before providing a sensible solution. Moreover the size of LN images is considerable. It follows that the improvement of computational efficiency can be an important issue.

A first attempt in this direction is proposed in [12] by remarking an analogy between a LN image and a projection in emission tomography. This remark suggests to apply the ordered subset expectation maximization (OSEM) method proposed by Hudson and Larkin [13] to the deconvolution of LN images.

The new algorithm consists in replacing the sum over the p images in (2) with a cycle over the same images. More precisely the algorithm is as follows:

- given $f^{(k)}$, set $h^{(0)} = f^{(k)}$ and, for $j = 1, 2, \ldots, p$, compute

$$h^{(j)} = h^{(j-1)} K_j^T * \frac{g_j}{K_j * h^{(j-1)} + b_j}. \tag{3}$$

- set $f^{(k+1)} = h^{(p)}$.

As shown in [13], such an approach provides a reduction in the number of iterations by a factor p, with approximately the same computational cost per iteration (a more accurate estimate is given in [12]). Since the number of detected images can be small, the improvement in efficiency with respect to the algorithm of (2) can be only by a factor between three and six. The improvement increases if the number of detected images increases; an interesting feature of this algorithm is that the computational time is approximately independent of the number of detected images.

THE RL ALGORITHM REQUIRES, IN GENERAL, A LARGE NUMBER OF ITERATIONS BEFORE PROVIDING A SENSIBLE SOLUTION.

However, in practice, a further improvement of efficiency can be desirable. To this purpose, one can use a rather general acceleration technique proposed by Biggs and Andrews [14]. This technique has been applied successfully to the algorithm of (3), with a reduction of the computational time of about 70% [8].

A theoretical difficulty with the previous algorithms is that convergence is not proved, even if it has always been found in all numerical experiments. Therefore it may be interesting to consider well founded acceleration methods such as the scaled gradient projection method proposed in [15]. This approach, however, can be applied to the algorithms of (1) and (2) but not to that of (3).

REGULARIZATION

As we already pointed out, early stopping of the iterations is required in all the previous algorithms to prevent excessive noise propagation. In other words, regularization is obtained by stopping the iterations even if, as far as we know, no sound stopping criterion is available in the case of RL. Therefore regularization may be required, also for taking into account special features of the scientific target (such as high dynamic range and edge-like structure). To this purpose, a Bayesian approach can be used [16].

In the maximum likelihood approach with Poisson noise, the maximization of the likelihood function is equivalent to the minimization of the Kullback-Leibler divergence, that is, a particular case of the Csiszár I-divergence [17]; the RL algorithm is just an iterative method converging to a minimizer of this divergence. In a Bayesian approach with Gibbs prior, the computation of the maximum a posteriori estimate leads to the minimization of a function that is obtained by adding a suitable penalization term to the Kullback-Leibler divergence. Classical regularizations can be obtained by means of the square of the Euclidean norm of the object and/or of its gradient, by means of its entropy, or by means of an edge-preserving penalty.

Iterative algorithms for the minimization of the penalized Kullback-Leibler divergence can be easily obtained by means of a general approach known as split-gradient method (SGM) [18]. They consist, in general, in a simple modification of the RL algorithm. Their extension to the OSEM method has been already proposed [16].

TWO ILLUSTRATIVE EXAMPLES

In this section, we consider two simple numerical examples. We do not simulate true observations with LN; therefore the PSFs are not extracted from the image, but ideal PSFs are used both for generating and deconvolving the images, corrupted by Poisson and Gaussian noise. In both examples we assume a good coverage of the u, v-plane, obtained by means of a few equi-spaced orientations of the baseline between 0° and 180°.

The first example is the binary of which two images are shown in Figures 2 and 3. Besides the images shown in the figures we generate two more images at 45° and 135°. All the images are 256×256. A background of 13.5 mag/arcsec^2 is also added. For the reconstruction we compare two methods: the coadding of (1) and the OSEM method of (3). At each iteration, the magnitude of the two stars is computed using a 3×3 square centered on each star. The behavior of the magnitudes as a function of the number of iterations is shown in Figure 4. It follows that both methods converge to the correct value but OSEM is much faster for the reasons discussed above. We just remark that on our PC, equipped with a 2.4 GHz Intel Core2Duo processor, the cost per iteration is 0.2355 s for OSEM and 0.0713 s for RL/coadding. However, for obtaining a magnitude of 20.1, we need only 20 OSEM iterations (4.7 s) while we need 360 RL/coadding iterations (25.7 s). Therefore OSEM provides a gain by a factor five.

The second example is the HST image of the Spirograph Nebula IC 418, reduced to an array 256×256, hence, to an angular size of about one arcsec, smaller than the true one by a factor 30. In such a case we generate six equispaced images, from 0° to 150°, assuming an integrated magnitude in K-band

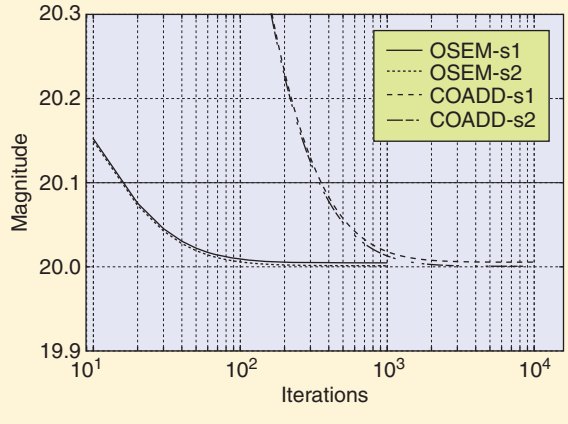

[FIG4] **Behavior of the magnitudes of the two stars, denoted *s*1, *s*2, as a function of the number of iterations for the two methods: OSEM and coadding.**

of ten and the same background of the previous example. We consider two cases: in the first we use only the images at 0°, 60°, and 120°; in the second all the six images. Again we compare OSEM and RL. At each iteration we compute the relative root mean square (rms) error between the reconstructed object and the original one. The behavior of this error, as a function of the number of iterations, is shown in Figure 5. We remark that the minimum of OSEM is reached after 30 iterations in the case of six images and after 70 iterations in the case of three images, while the minimum of the coadding is reached respectively after 240 and 230 iterations. We can conclude that, for both methods, the computational time is approximately independent of the number of interferometric images.

In this second example, we find that OSEM is not only faster but also provides a smaller reconstruction error, even if the improvement with respect to the coadding method is not very significant. We also find that the use of six images instead of three does not improve the reconstruction in a very relevant way, as shown in Figure 6.

In the previous examples, we assumed the same integration time for all images so that they have approximately the same flux and the same SNR. We remark that, if we increase the number of images, then we increase the global SNR. However, such an increase has no influence on the computational time. This is controlled by the SNR of a single image. If this is decreased (for instance by decreasing the integration time), then the computational time also decreases while the reconstruction error increases.

A THEORETICAL DIFFICULTY WITH THE PREVIOUS ALGORITHMS IS THAT CONVERGENCE IS NOT PROVED, EVEN IF IT HAS ALWAYS BEEN FOUND IN ALL NUMERICAL EXPERIMENTS.

OTHER TOPICS AND CONCLUSIONS

The previous examples illustrate the best results achievable with LN. The reconstruction may be degraded by an incomplete coverage of the u, v-plane or by a low Strehl ratio (SR) and low uniformity of the AO correction [3]. The effect of low SR is taken into account in [19] where the reconstruction of two scientific targets is investigated. An open problem is how stopping criteria are chosen in practice.

The previous algorithms can be used if the scientific target is completely contained within the image domain. Otherwise, one must take into account boundary effects. A simple method for reducing these effects is proposed in [20] and [21] and is used in [8]. Moreover, the improvement of the extracted PSFs can require the use of a semiblind approach [22]. Work is in progress for applying to LN a recently proposed iterative semiblind method, using a constraint on the SR of the PSF [23].

All methods are implemented in the software package Astronomical Image Restoration in Interferometry (AIRY) version 4.0, developed by our group for simulation and reconstruction of LN images. It is CAOS-based (see http://fizeau.unice.fr/caos for more information) and is developed and publicly distributed since 2002 (see http://www.airyproject.eu). AIRY-LN, version 1.0 [24], conceived as a specific adaptation of our more general tool AIRY [25], is one of a collection of various numerical tools being developed in support of the astrophysical observations made with LN.

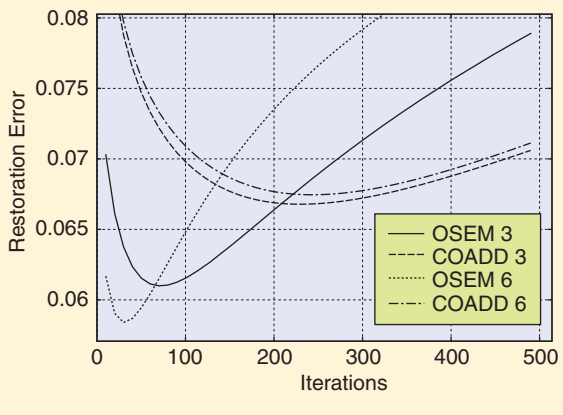

[FIG5] **Behavior of the relative rms error in the reconstruction of the image of the Spirograph Nebula as a function of the number of iterations, for the two methods considered and in the case of three or six images.**

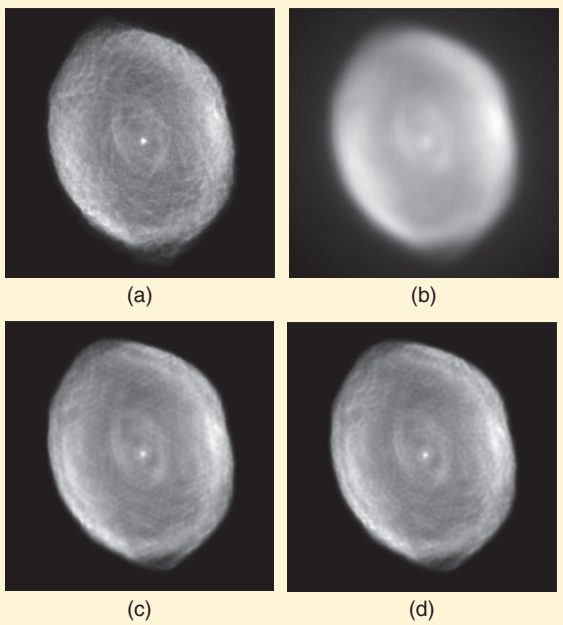

[FIG6] **(a) Original image of the Spirograph Nebula; (b) LN-image corresponding to 0°; the reconstructions provided by OSEM with (c) three and (d) six images.**

AUTHORS

Mario Bertero (bertero@disi.unige.it) is a professor of information science with the Department of Computer Science of the University of Genova. He received the BcS degree in physics in 1960 and the "libera docenza" in theoretical physics in 1968. From 1989 to 1994, he was editor of *Inverse Problems*. He is author and coauthor of more than 150 papers and coauthor of one book. His main research interests are in the theory and practice of inverse problems, including regularization and Bayesian approaches, analytic and numerical methods, applications to image reconstruction in astronomy, microscopy, medical imaging, and geo-science.

Patrizia Boccacci (boccacci@disi.unige.it) received the advanced degree in physics from the University of Genova in 1980. Since 2004, she has been an associate professor in the Department of Computer and Information Sciences of the University of Genova. She is author and coauthor of about 100 papers and coauthor of one book. Her main research interest is in numerical methods for the solution of inverse problems and their applications, such as optical tomography for the investigation of crystal growth in microgravity, confocal microscopy, particle sizing, seismic tomography, and astrophysics. More recently, her research interest is in image restoration problems related to the LBT project and in medical imaging.

Gabriele Desiderà (desidera@disi.unige.it) is a Ph.D. student in at the University of Genova. His research interest is in inverse problems related to astronomical imaging, particularly on image restoration problems for ground-based telescopes. In the framework of the LINC-NIRVANA consortium, he contributes to the development and maintenance of the AIRY Software Package, a software product created to perform astronomical image reconstruction, as well as of AIRY-LN, an ad hoc version to support LINC-NIRVANA.

Andrea La Camera (lacamera@disi.unige.it) received the advanced degree in physics from the University of Genova in 2006. From 2006 to 2008, he collaborated on the development of the software packages AIRY and AIRY-LN. Since 2008, he has been a Ph.D. student at the University of Genova. His research interests are in image denoising and restoration with application to infrared astronomy and medical imaging.

Marcel Carbillet (marcel.carbillet@unice.fr) received the Ph.D. degree in 1996 from the University of Nice-Sophia Antipolis (UNS), France, in the field of optical astronomy (speckle imaging techniques of binary/multiple stars). He spent one year at the University of Geneva, Switzerland, working on atmospheric optics, and seven years at Osservatorio Astrofisico di Arcetri, Florence, Italy, working on adaptive optics and Fizeau interferometry imaging with the large binocular telescope. He is currently maître de conférence with the Fizeau laboratory (UNS/CNRS/OCA), focusing mainly on AO, high angular resolution imaging (especially post-AO data), and high contrast imaging techniques (especially concerning exoplanets).

Henri Lantéri (henri.lanteri@unice.fr) is a professor (emeritus) at the University of Nice-Sophia Antipolis, France, with the Fizeau laboratory (UNS/CNRS/OCA). His research is focused on inverse problems, mainly on image reconstruction algorithms in the field of astronomical images.

REFERENCES

[1] J. R. P. Angel, "Sensitivity of optical interferometers with coherent image combination," *Proc. SPIE*, vol. 4838, pp. 126–133, 2003.

[2] W. Gaessler, C. Arcidiacono, S. Egner, T. M. Herbst, D. Andersen, H. Baumeister, P. Bizenberger, H. Boehnhardt, F. Briegel, M. Kuester, W. Laun, L. Mohr, B. Grimm, H.-W. Rix, R.-R. Rohloff, R. Soci, C. Stroz, W. Xu, R. Ragazzoni, P. Salinari, E. Diolaiti, J. Farinato, M. Carbillet, L. Schreiber, A. Eckart, T. Bertram, C. Strubmeier, Y. Wang, L. Zealouk, G. Weigelt, U. Beckmann, J. Behrend, T. Driebe, M. Heininger, K.-H. Hofmann, E. Nussbaum, D. Shertel, E. Masciadri "LINC-NIRVANA: MCAO toward extremely large telescopes," *C. R. Physique*, vol. 6, no. 10, pp. 1129–1138, 2005.

[3] M. Carbillet, S. Correia, P. Boccacci, and M. Bertero, "Restoration of interferometric images. II. The case-study of large binocular telescope," *Astron. Astrophys.*, vol. 387, no. 2, pp. 744–757, 2002.

[4] W. H. Richardson, "Bayesian-based iterative method of image restoration," *J. Opt. Soc. Amer.*, vol. 62, pp. 55–59, 1972.

[5] L. Lucy, "An iterative technique for the rectification of observed distribution," *Astron. J.*, vol. 79, pp. 745–775, 1974.

[6] L. A. Shepp and Y. Vardi, "Maximum likelihood reconstruction in positron emission tomography," *IEEE Trans. Med. Imag.*, vol. 1, pp. 113–122, 1982.

[7] M. Bertero and P. Boccacci, *Introduction to Inverse Problems in Imaging*. Bristol, U.K.: IoP Publishing, 1998.

[8] A. La Camera, G. Desiderà, C. Arcidiacono, P. Boccacci, and M. Bertero, "Advances in the reconstruction of LBT LINC-NIRVANA images," *Astron. Astrophys.*, vol. 471, no. 3, pp. 1091–1097, 2007.

[9] B.Anconelli, M. Bertero, P. Boccacci, M. Carbillet, and H. Lanteri, "Restoration of interferometric images. III. Efficient Richardson-Lucy methods for LINC-NIRVANA data reduction," *Astron. Astrophys.*, vol. 430, no. 2, pp. 731–738, 2005.

[10] K.-H. Hofmann, T. Driebe, M. Heininger, D. Schertl, and G. Weigelt, "Reconstruction of aperture-synthesis images from LBT LINC-NIRVANA data using the Richardson-Lucy and space-variant building-block method," *Astron. Astrophys.*, vol. 444, no.3, pp. 983–993, 2005.

[11] D. G. Politte and D. L. Snyder, "Correction for accidental coincidences and attenuation in maximum-likelihood image reconstruction for positron-emission tomography," *IEEE Trans. Med. Imag.*, vol. 10, pp. 82–89, 1991.

[12] M. Bertero and P. Boccacci, "Application of the OS-EM method to the restoration of LBT images," *Astron. Astrophys. Suppl. Ser.*, vol. 144, no.1, pp. 181–186, 2000.

[13] H. M. Hudson and R. S. Larkin, "Accelerated image reconstruction using ordered subsets of projected data," *IEEE Trans. Med. Imag.*, vol. 13, pp. 601–609, 1994.

[14] D. S. C. Biggs and M. Andrews, "Acceleration of iterative image restoration algorithms," *Appl. Optics*, vol. 36, pp. 1766–1775, 1997.

[15] S. Bonettini, R. Zanella, and L. Zanni, "A scaled gradient projection method for constrained image deblurring," *Inverse Problems*, vol. 25, no. 1, 015002, 2009.

[16] B. Anconelli, M. Bertero, P. Boccacci, M. Carbillet, H. Lanteri, and S. Correia, "Deconvolution methods for LINC-NIRVANA data reduction," in *Proc. SPIE* (New Frontiers in Stellar Interferometry, vol. 5491), W. A. Traud, Ed. 2004, pp. 932–943.

[17] I. Csiszár, "Why least squares and maximum entropy? An axiomatic approach to inference for linear inverse problems," *Ann. Stat.*, vol. 19, no. 4, pp. 2032–2066, 1991.

[18] H. Lanteri, M. Roche, and C. Aime, "Penalized maximum likelihood image restoration with positivity constraints: Multiplicative algorithms," *Inverse Problems*, vol. 18, pp. 1397–1419, 2002.

[19] P. Ciliegi, A. La Camera, G. Desiderà, S. Antoniucci, C. Arcidiacono, M. Lombini, E. Diolaiti, E. Bellocchi, F. Mannucci, M. Bertero, P. Boccacci, D. Lorenzetti, and B. Nisini, "Analysis of LBT LINC-NIRVANA simulated images of galaxies and young stellar objects," *Proc. SPIE*, vol. 7013, 701335, 2008.

[20] M. Bertero and P. Boccacci, "A simple method for the reduction of boundary effects in the Richardson-Lucy approach to image deconvolution," *Astron. Astrophys.*, vol. 437, no.1, pp. 369–374, 2005.

[21] B. Anconelli, M. Bertero, P. Boccacci, M. Carbillet, and H. Lanteri, "Reduction of boundary effects in multiple image deconvolution with an application to LBT LINC-NIRVANA," *Astron. Astrophys.*, vol. 448, no. 3, pp. 1217–1224, 2006.

[22] G. Desiderà, B. Anconelli, M. Bertero, P. Boccacci, and M. Carbillet, "Application of iterative blind deconvolution to the reconstruction of LBT LINC-NIRVANA images," *Astron. Astrophys.*, vol. 452, no. 2, pp. 727–743, 2006.

[23] G. Desiderà and M. Carbillet, "Strehl-constrained iterative blind deconvolution for post-adaptive-optics data," *Astron. Astrophys.*, to be published.

[24] G. Desiderà, A. La Camera, M. Bertero, P. Boccacci, and M. Carbillet, "AIRY-LN: An ad-hoc numerical tool for deconvolution image from the LBT instrument LINC-NIRVANA," *Proc. SPIE*, vol. 7013, 701340, 2008.

[25] S. Correia, M. Carbillet, P. Boccacci, M. Bertero, and L. Fini, "Restoration of interferometric images. I. The software package AIRY," *Astron. Astrophys.*, vol. 387, no. 2, pp. 733–743, 2002. [SP]